METALS AND MATERIALS International, Vol. 7, No. 2 (2001), pp. 91~94

Nanocrystallization and High Tensile Strength of Amorphous Zr-Al-Ni-Cu-Ag Alloys

T. K. Han, S. J. Kim*,Y. S. Yang*, A. Inoue, Y. H. Kim and I. B. Kim**

Department of Metallurgical Engineering, Pusan National University
San 30 Changjeon-dong, Keumjeong-ku, Pusan 609-735, Korea
*Research Center for Dielectric and Advanced Matter Physics, Pusan National University
**Institute for Materials Research, Tohoku University, Sendai 980-8577, Japan

The influence of the addition of Ag to the crystallization and mechanical properties of the amorphous $Zr_{65}Al_{7.5}Ni_{10}Cu_{17.5-x}Ag_x$ (x=5, 10 at.%) alloys was investigated. It was found that crystallization takes place through the two-stage process of Am→Am'+icosahedral→phase Zr_2Cu+Zr_2Ni+Zr_2Al_3. The icosahedral particles have a spherical morphology and their sizes range from 10 to 100 nm. With the increase in the amount of Ag, thermal instability increases through the simultaneous decrease of T_x and ΔT_x. The σ_f increases significantly from 1560 MPa at 0%V_f to 2120 MPa at 62%V_f for the 10% Ag alloy.

Keywords : amorphous alloy, nanocrystallization, icosahedral phase, mechanical property

1. INTRODUCTION

It is well known that the Zr-based amorphous alloys have good mechanical properties compared with conventional crystalline alloys such as high tensile strength, high bending strength, high Charpy impact energy and high fatigue strength [1]. Also, it has been reported that the tensile fracture strength of the Zr-based amorphous alloys increases further in the coexistent structures of amorphous and nanoscale compound particles [2-3]. The nanocrystallization of amorphous alloy has attracted great interest because nanoparticles can be synthesized through partial crystallization of the amorphous phase.

It has been reported recently that the icosahedral phase precipitates as the primary precipitation phase in the Zr-Al-Cu-Ni [4] and Zr-Al-Cu-Ni-Ti [5] amorphous alloys and induces improvement in the mechanical properties of hardness and tensile strength. Quite recently, we have found that the nanoscale icosahedral quasicrystalline particles precipitate homogeneously in amorphous Zr-Al-Ni-Cu-Ag alloy [6].

In the present paper, the nanocrystallization behavior and mechanical properties of the amorphous $Zr_{65}Al_{7.5}Cu_{17.5-x}Ni_{10}Ag_x$ (x=5, 10) alloys are investigated. We try to interpret the enhancement of mechanical strength from the perspective of the bonding force between atomic pairs.

2. EXPERIMENTAL PROCEDURE

Multicomponent alloys with the composition of $Zr_{65}Al_{7.5}Ni_{10}Cu_{17.5-x}Ag_x$ (x=5, 10 at.%) were examined in this study. Their alloy ingots were prepared by arc melting mixtures of pure metals in a purified argon atmosphere. Ribbon samples with a cross section of about 0.03×1.2 mm^2 were produced by the single roller melt spinning method. Annealing was performed in an IR furnace with a near-infrared lamp in an argon atmosphere for 140 s to 600 s in temperatures ranging from 683 to 873 K. IR heating is useful for rapid heating and cooling. The thermal properties were measured by differential scanning calorimetry at a heating rate of 0.67 Ks^{-1}. The structures of the melt-spun state and annealed state were investigated by X-ray diffractometry and transmission electron microscopy. Mechanical properties were measured by Vickers microhardness under a load of 0.98 N(100 gf) and a tensile test at a strain rate of 8.33×10^{-4} s^{-1} with an Instron testing machine. The fracture surface morphology was examined by scanning electron microscopy.

3. RESULTS AND DISCUSSION

Fig. 1 shows the DSC curves of the melt-spun $Zr_{65}Al_{7.5}Ni_{10}Cu_{17.5-x}Ag_x$ (x=5(5%Ag alloy), 10(10%Ag alloy) at.%) amorphous alloys. It has been reported that the amorphous $Zr_{65}Al_{7.5}Ni_{10}Cu_{17.5}$ (0%Ag alloy) alloy crystallizes through a single stage due to Zr_2Cu, Zr_2Ni, Zr_2Al_3 and ZrNi phases [7]. However, the Ag addition changes the crystallization process into a two-stage process. As the amount of Ag increases, T_g (glass transition temperature) increases but T_x (crystallization onset temperature) decreases, resulting in a decrease of ΔT_x

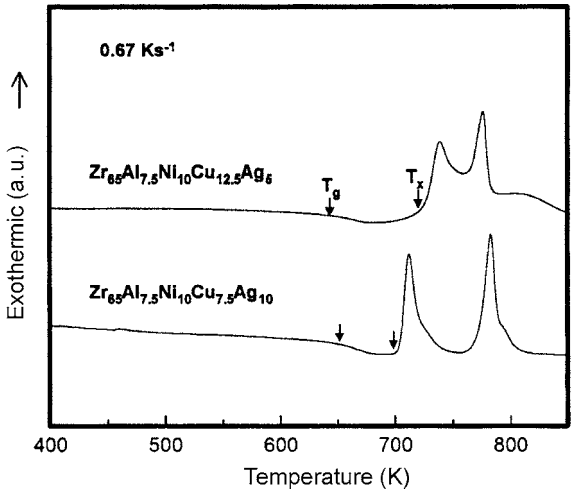

Fig. 1. DSC curves of amorphous $Zr_{65}Al_{7.5}Ni_{10}Cu_{17.5-x}Ag_x$ (x=5, 10 at.%) alloys with heating rate of 40 Ks^{-1}. (T_g: glass transition temperature, T_x: crystallization onset temperature).

(supercooled liquid region). This result indicates that thermal instability increases with increasing Ag content. Although the thermal instability increases, the supercooled liquid region exceeding 50 K is maintained for the 10%Ag alloy.

In order to clarify the crystallization behavior, the XRD patterns of the 5%Ag and 10%Ag alloys, annealed 150 s at each exothermic temperature of DSC, are shown in Fig. 2. It was confirmed that the first exothermic peak was due to the

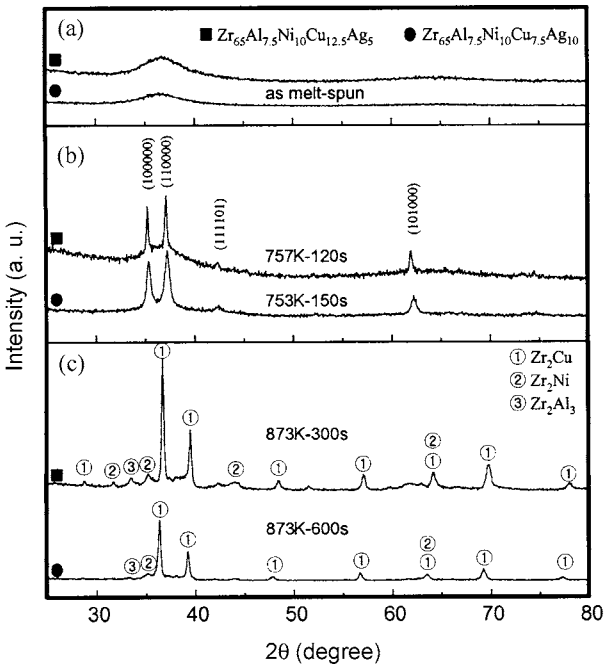

Fig. 2. X-ray patterns of amorphous $Zr_{65}Al_{7.5}Ni_{10}Cu_{17.5-x}Ag_x$ (x=5, 10 at.%) alloys annealed for shown aging time at several aging temperatures.

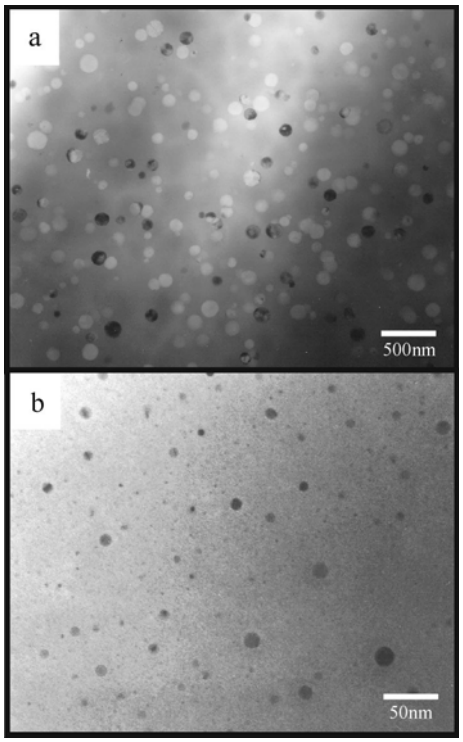

Fig. 3. Bright-field TEM images of (a) $Zr_{65}Al_{7.5}Ni_{10}Cu_{12.5}Ag_5$ alloy annealed 180 s at 757 K with 55% V_f and (b) $Zr_{65}Al_{7.5}Ni_{10}Cu_{7.5}Ag_{10}$ alloy annealed 150 s at 723 K with 53% V_f.

precipitation of an icosahedral phase (Fig. 2(b)) from the supercooled liquid region and that the second was due to the precipitation of Zr_2Cu, Zr_2Ni, Zr_2Al, ZrAl and Zr_2Ag crystals (Fig. 2(c)). We have not included the diffraction pattern of the selected area for the precipitates but it was previously confirmed to be the icosahedral phase [5]. It was, therefore ,concluded that the crystallization process occurs in a two stage process (Figs. 2(a)-(c)) consisting of Am→Am'+icosahedral phase→Zr_2Cu+Zr_2Ni+Zr_2Al_3.

Fig. 3 shows the bright-field TEM images of (a) $Zr_{65}Al_{7.5}Ni_{10}Cu_{12.5}Ag_5$ alloy annealed 180 s at 757 K with 55% V_f and (b) $Zr_{65}Al_{7.5}Ni_{10}Cu_{7.5}Ag_{10}$ alloy annealed 150 s at 723 K with 53% V_f. The volume fraction, V_f of the icosahedral phase was calculated from the formula: $V_f=(\Delta H_{\text{as melt-spun}}-\Delta H_{\text{heat treated}})/(\Delta H_{\text{as melt-spun}})\times 100(\%)$, where ΔH is the crystallization heat (enthalpy change) and corresponds to the first peak area of the DSC curve.

It may be seen that all the precipitates have a spherical morphology. The sizes and the interparticle spacing of particles measure from a range of 50 to 100 nm and 50 nm, respectively, for the 5%Ag alloy and 10 to 20 nm and 25 nm, respectively, for the 10%Ag alloy. This result indicates that the growth rate of the icosahedral phase for the 5%Ag alloy is faster than that of the 10%Ag alloy at the same V_f. Moreover, the difference in particle size and interparticle spacing of similar V_f between the 5%Ag alloy and 10%Ag alloy is likely to

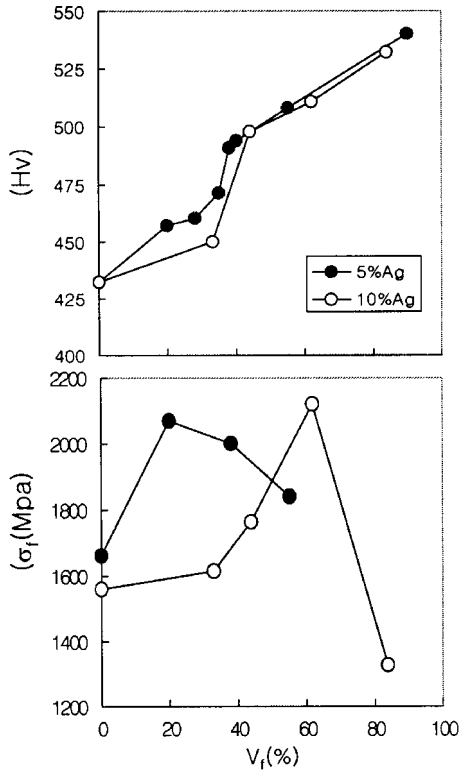

Fig. 4. Vickers hardness (*Hv*) and tensile fracture strength (σ_f) as a function of volume fraction (V_f) of icosahedral phase or compounds for the amorphous $Zr_{65}Al_{7.5}Ni_{10}Cu_{17.5-x}Ag_x$ (x=5, 10 at.%) alloys.

induce the difference in mechanical properties.

Fig. 4 shows Vickers hardness (*Hv*) and tensile fracture strength (σ_f) as a function of the volume fraction of the icosahedral phase for $Zr_{65}Al_{7.5}Ni_{10}Cu_{17.5-x}Ag_x$ alloy (x=5, 10 at.%) annealed for different periods at various temperatures. The *Hv* increases linearly with increasing V_f in all alloys but the *Hv* of the 10%Ag alloy is somewhat higher than that of 5%Ag alloy. However, the σ_f significantly increases from 1660 to 2070 MPa at V_f=20% for the 5%Ag alloy and from 1560 to 2120 MPa at V_f=62% for the 10%Ag alloy. The σ_f decreases as the V_f further increases.

Here, we will consider the reason why the σ_f of the 5%Ag alloy is higher than that of the 10%Ag alloy in the wide V_f range. This will be discussed on the basis of the strength of the amorphous matrix itself. The replacement effect of Cu by Ag can be explained by the difference in the bonding force between the Zr and Cu or Ag atoms in the amorphous matrix. The Zr-Ag pair is expected to have a weaker bonding force than the Zr-Cu pair [8]. This presumption is supported by the decrease of T_x and σ_f. This result indicates that the difference in σ_f in both alloys must be explained by considering the differences in the bonding forces between the Zr and Cu or Ag atoms.

Fig. 5 shows the tensile fracture surface of the 10%Ag alloy with different V_f. As shown in Fig. 5(a), the fracture surface of the amorphous single phase is typically composed of two zones, i.e., a smooth region caused by shear deformation and a vein region caused by final fracture after shear deformation. With the increase in V_f (Fig. 5(a)-(c)), the fracture surface consists of a well-developed vein pattern which is typical for ductilization and fracture takes place along the maximum shear plane declining by about 45 degrees in the direction of the tensile load. This difference in fracture suggests that the nanoscale icosahedral particles act as an effective barrier to shear deformation and enhance the degree of local adiabatic heating, leading to the more significant viscous flow of the amorphous matrix. However, Fig. 5(d) shows that the fracture mode changes from the shear type mode to a mixed type of shear- and perpendicular- mode in the higher V_f range above 62%, accompanying the decreases in σ_f.

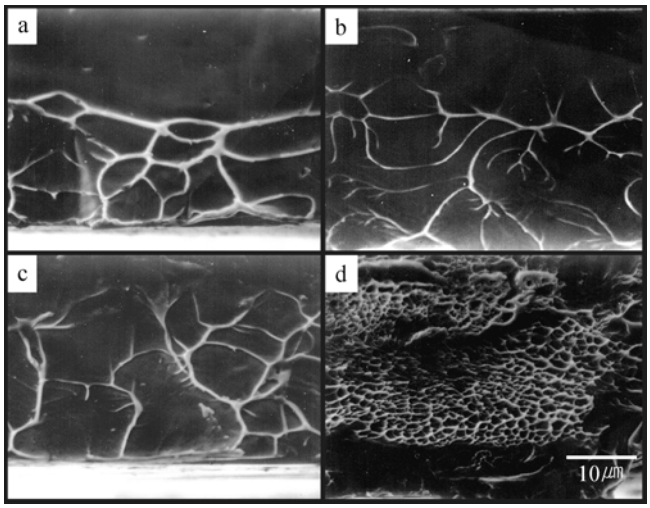

Fig. 5. Tensile fracture surface of the $Zr_{65}Al_{7.5}Ni_{10}Cu_{7.5}Ag_{10}$ alloy with different V_f: (a) 0%, (b) 44%, (c) 62% and (d) 84%.

We will now discuss the reason why the icosahedral base alloys have high mechanical strength and good ductility. It is well known that the icosahedral alloys with stoichiometric compositions have high levels of hardness and are extremely brittle at room temperature [9]. It is thought that the good ductility and high mechanical strength are obtained through a combination of the ductility of the amorphous matrix and the high levels of hardness of the icosahedral phase. Also, it is well known that deformation of the amorphous alloys at room temperature occurs along the maximum shear plane through the massive movement of constituent atoms within a width of 20 to 30 nm [10, 11]. This result implies that the nanoscale rigid icosahedral particles can act as an effective barrier to the shear deformation of the amorphous matrix. And the decrease in σ_f is considered to occur when the ductile-brittle transition takes place.

4. SUMMARY

We have examined the influence of the element Ag on the crystallization behavior and mechanical properties of $Zr_{65}Al_{7.5}Ni_{10}Cu_{17.5-x}Ag_x$ (x=5, 10 at.%) alloys. It was found that crystallization takes place through a two-stage process: Am →Am'+icosahedral phase→Zr_2Cu Zr_2Ni Zr_2Al_3. The icosahedral particles have a spherical morphology and their sizes are 50 to 100 nm for the 5%Ag alloy and 10 to 20 nm for the 10%Ag alloy. As the amount of Ag increases, the thermal instability increases through the simultaneous decrease of T_x and ΔT_x. The σ_f increases significantly from 1660 MPa at 0% V_f to 2070 MPa at 20% V_f for the 5%Ag alloy and from 1560 MPa at 0% V_f to 2120 MPa at 62% V_f for the 10%Ag alloy. The significant increase in σ_f is due to the fact that the rigid nanoscale icosahedral particles embedded in the ductile amorphous matrix can act as a barrier to the shear deformation of the amorphous matrix.

ACKNOWLEDGMENT

The authors wish to acknowledge the financial support of the Korea Research Foundation made in the program year 1997(1997-011-E00033). This work was supported by Pusan National University (PNU), PNU Research Grant 1999. We lost Prof. Y. H. Kim during this research and express our deepest sympathy to his family.

REFERENCES

1. A. Inoue, *Bulk Amorphous Alloys*, Trans Tech Publications, Zurich (1998).
2. A. Inoue, T. Zhang and Y. H. Kim, *Mater. Trans. JIM* **38**, 749 (1997).
3. G. C. Koch, D. G. Morris, K. Lu and A. Inoue, *MRS Bul.* **24**, 54 (1999).
4. U. Kster, J. Meinhardt, S. Roos and H. Liebertz, *Appl. Phys. Lett.* **69**, 179 (1996).
5. L. Q. Xing, J. Eckert, W. Loser and L. Schultz, *Appl. Phys. Lett.* **73**, 2110 (1998).
6. A. Inoue. T. Zhang, M. Wei Chen and T. Sakurai, *Mater. Trans. JIM* **12**, 1382 (1999).
7. A. Inoue, D. Kawase, A. P. Tsai, T. Zhang and T. Masumoto, *Mater. Sci. Eng. A* **178**, 255 (1994).
8. F. R. de Boer, R. Boom, W. C. M. Mattens, A. R. Miedema and A. K. Niessen, *Cohesion in Metals,* p. 298, Elsevier Science, Amsterdam (1998).
9. S. Takeuchi, *Quasicrystals*, p. 125, Tokyo (1992).
10. T. Masumoto and R. Maddin, *Acta metall.* **19**, 725(1971).
11. J. C. M. Li, *Rapidly Solidified Alloys*, p. 379, Marcel Dekker, Inc., New York (1993).